Comparison of asymptotics of heart and nerve excitability

Rebecca Suckley and Vadim N. Biktashev
Department of Mathematical Sciences, Liverpool University, Mathematics and Oceanography Building, Peach Street, Liverpool L69 7ZL, United Kingdom
(Received 11 February 2003; published 11 July 2003)

We analyze the asymptotic structure of two classical models of mathematical biology, the models of electrical action by Hodgkin-Huxley (1952) for a giant squid axon and by Noble (1962) for mammalian Purkinje fibres. We use the procedure of parametric embedding to formally introduce small parameters in these experiment-based models. Although one of the models was designed as a modification of the other, their structure with respect to the small parameters appears to be entirely different: the Hodgkin-Huxley model has two slow and two fast variables, while Noble's model has one slow variable, two fast variables, and one superfast variable. The singular perturbation theory of these models adequately reproduces some features of the accurate numeric solutions, such as excitability and the shape of the voltage upstroke, but fails to reproduce other features, such as the relatively slow return from the excited state, compared to the speed of the upstroke. We present arguments towards the viewpoint that contrary to the conjecture proposed by Zeeman (1972), for these two models this failure is an inevitable consequence of the Tikhonov-style appearance of the small parameters, and a more adequate asymptotic description may only be achieved with small parameters entering the equations in a significantly different way.

DOI: 10.1103/PhysRevE.68.011902 PACS number(s): 87.10.+e

I. INTRODUCTION

The idea of the present study came from a 1972 paper by Zeeman [1], which was one in his series of works dedicated to possible applications of the then new catastrophe theory [2]. In that paper, Zeeman has analyzed an apparent difference between two sorts of biological excitable systems, nerve and heart, and conjectured that this difference may come as a consequence of them being described by singularly perturbed systems of equations, with the slow manifolds demonstrating catastrophes of different types. Amazingly, in the following 30 years, there were no published papers directly testing this conjecture. To fill in this gap, was one reason to undertake this study.

The other reason was more practical. Mathematical models describing biological excitable systems, particularly nerve and heart tissues, are historically the first, and so far the best, in terms of quantitative description of truly biological phenomena, based on solid experimental information. A special place in this set belongs to Hodgkin and Huxley's [3] model of the squid giant axon, and Noble's [4] model of the cells of Purkinje fibres of mammalian heart. These were historically the first and still the simplest in that family. Since then, the progress in development of realistic models of different kinds of cells has been enormous, and the current models achieve remarkable complexity and accuracy, particularly for cardiac cells [5,6]. One disappointing, from a theoretical physicist's point of view, feature of all these models is a seemingly absolute necessity of numerical treatment, since they are high-order [at least, of order 4, as for both the Hodgkin-Huxley (HH) and Noble-1962 (N62) models] nonlinear systems of differential equations, and do not admit exact analytical solution. Purely numerical study, however good the computers may be, always has well known disadvantages, e.g., lack of insight into dependence of the solutions on the parameters. Thus, from the very beginning there were attempts to understand the behavior of the solutions in these models by some asymptotic methods, and to devise simpler models that admit analytical treatment. The most prominent example of such study was the paper by FitzHugh [7], who has shown that a modification of Van der Pol's nonlinear oscillator can demonstrate qualitative properties very similar to those of the HH system, and that a collection of appropriate two-dimensional projections of the four-dimensional trajectories of the HH system look similar to the phase portrait of the modified Van der Pol system. When considered as a singularly perturbed system, FitzHugh's system allowed a qualitative analysis explaining its main features *without using a computer*. Ever since, FitzHugh's system and its numerous variations are very popular as simple systems qualitatively similar to real excitable systems, and allowing both a better qualitative understanding, and a more efficient numerical treatment of large numbers of excitable cells, than detailed, realistic models. Yet, these simplified models are only in qualitative and not in quantitative agreement with the real systems. Moreover, these simplified models are not in any way *derived* from the realistic systems, and therefore there is no way to be sure that they reproduce even the qualitative effects correctly.

This makes a case for deriving simplified models from realistic models, by exploiting their real properties, via a clearly defined set of assumptions and transformations. One such attempt was made as early as 1973 by Krinsky and Kokoz [8] who have considered the HH system as a singularly perturbed system to reduce its order to 3, and an *ad hoc* empirical observation to further reduce it to 2, which ended up with a system whose phase portrait looked similar to that of FitzHugh's system, but already without any small parameters left. Although very interesting in a historical perspective, that paper failed to have a more lasting impact in its time, in particular, because the *ad hoc* methods used there could not be transferred to more sophisticated models.

TABLE I. Parameters and functions of the Hodgkin-Huxley and Noble-1962 models.

Parameter or function	Hodgkin-Huxley system	Noble-1962 system
C_M	1	12
$\alpha_m(E)$	$\frac{0.1(-E+25)}{e^{(-E+25)/10}-1}$	$\frac{0.1(-E-48)}{(e^{(-E-48)/15}-1)}$
$\alpha_n(E)$	$\frac{0.01(-E+10)}{(e^{(-E+10)/10}-1)}$	$\frac{0.0001(-E-50)}{(e^{(-E-50)/10}-1)}$
$\alpha_h(E)$	$0.07e^{-E/20}$	$0.17e^{(-E-90)/20}$
$\beta_m(E)$	$4e^{-E/18}$	$\frac{0.12(E+8)}{(e^{(E+8)/5}-1)}$
$\beta_n(E)$	$0.125e^{-E/80}$	$0.002e^{(-E-90)/80}$
$\beta_h(E)$	$\frac{1}{(e^{(-E+30)/10}+1)}$	$\frac{1}{(e^{(-E-42)/10}+1)}$
$\bar{g}_{\mathrm{Na}}$	120	400
$\bar{g}_{\mathrm{Na}_1}$	0	0.14
$\bar{g}_{\mathrm{K}}$	36	1.2
$\bar{g}_{\mathrm{K}_1}(E)$	0	$1.2e^{(-E-90)/50}$ $+0.015e^{(E+90)/60}$
$\bar{g}_l$	0.3	0
E_{Na}	115	40
E_{K}	-12	-100
E_l	10.613	-60

With the advent of computational biology of extended biological systems including large numbers of excitable elements, such as large neural networks or whole heart, the question of faithful simplifications of detailed models gains more and more of practical importance. Various kinds of simplified models of excitable systems, such as FitzHugh and its variations, and even further caricaturelike simplifications, such as integrate-and-fire neurons, cellular automata, etc., have been used in large scale computations as a ''poor man's substitute'' of realistic models. Now the level of understanding achievable at such caricature level is to a considerable extent exhausted. On the other hand, the development of computer technology itself has not been in pace with the demand from applications, e.g., in biomedical engineering in cardiology. There have been several attempts to develop models which would mimic the properties of realistic models but would be less computational expensive, see, e.g., Refs. [9–12]. However, all these attempts so far have been, at least in some points, phenomenological, and thus have the same principal disadvantages as FitzHugh's attempt, i.e., lack of confidence in quantitative and perhaps even qualitative predictions. Hence, development of methods of reliable and verifiable derivation of simplified models, qualitatively and quantitatively reproducing relevant properties of the detailed models, or deviating from them in a controllable way, can present a considerable advantage for computations for applications. We believe that the methods of such derivations should be developed starting from the simplest cases, and then generalized to more sophisticated models. The present paper deals with the two simplest cases.

The structure of this paper is as follows. In Sec. II, we introduce Hodgkin and Huxley's (1952) and Noble's (1962) systems of equations. In Sec. III, we present the relevant bits of the singular perturbation theory of fast-slow systems, such as the concepts of fast foliation and slow manifold. Section IV describes two Zeeman's toy models and their analysis, as an illustration of the method we use later for the HH and N62 models. Section V describes parametric embedding, the formal procedure of introducing artificial small parameters to enable asymptotic treatment of experiment-based models, which do not have parameters but only experimentally measured constants. In Sec. VI, we analyze the relative speeds of the four variables in both the HH and N62 models, to assign them the roles of slow and fast variables. The main results are presented in Secs. VII and VIII, where we apply all the described methods to the HH and N62 models. The discussion of the results is presented in Sec. IX.

II. HOGKIN-HUXLEY'S 1952 AND NOBLE'S 1962 SYSTEMS OF EQUATIONS

Both the HH and N62 systems of equations can be written in the same form,

$$\frac{dE}{dt}=C_M^{-1}f_E(E,h,m,n),$$

$$\frac{dh}{dt}=\alpha_h(E)(1-h)-\beta_h(E)h=[\bar{h}(E)-h]/\tau_h(E),$$

$$\frac{dm}{dt}=\alpha_m(E)(1-m)-\beta_m(E)m=[\bar{m}(E)-m]/\tau_m(E),$$

$$\frac{dn}{dt}=\alpha_n(E)(1-n)-\beta_n(E)n=[\bar{n}(E)-n]/\tau_n(E), \quad (1)$$

where

$$f_E(E,h,m,n)=[\bar{g}_{\mathrm{K}}n^4+\bar{g}_{\mathrm{K}_1}(E)](E_{\mathrm{K}}-E)+(\bar{g}_{\mathrm{Na}}m^3h+\bar{g}_{\mathrm{Na}_1})\times(E_{\mathrm{Na}}-E)+\bar{g}_l(E_l-E)$$

is the total current passing through the membrane measured in $\mu\mathrm{A/cm}^2$, t is time measured in milliseconds, E is the transmembrane voltage measured in millivolts, E_k, $k=\mathrm{Na,K},l$ are the reversal potentials of sodium, potassium, and leakage currents, respectively, measured in the same scale as E, $\bar{g}_k$ are corresponding maximal specific conductances in $\mathrm{mmho/cm}^2$, n, m, h are dimensionless ''gating'' variables, C_M is the specific membrane capacitance in $\mu\mathrm{F/cm}^2$, $\alpha_j(E)$, $\beta_j(E)$, $j=h,m,n$, are gate's opening and closing rates in ms^{-1}, $\bar{j}(E)=\alpha_j/(\alpha_j+\beta_j)$ are the gates' instant equilibrium values, and $\tau_j(E)=1/(\alpha_j+\beta_j)$ are the gates' dynamics time scales in milliseconds. The standard values of parameters and forms of the functions used in Eq. (1) are different for the HH and N62 models, and are summarized in Table I.

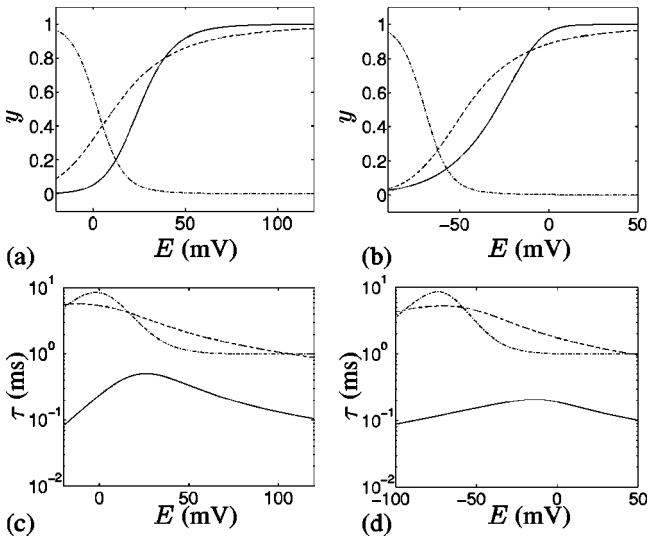

FIG. 1. Properties of the channel gates' in the Hodgkin-Huxley (HH) system and Noble-1962 (N62) system. (a,b) The quasistationary values of the gates $y=\bar{m},\bar{h},\bar{n}$ in the HH (a) and N62 (b) systems. Solid lines, $\bar{m}(E)$; dash-dotted lines, $\bar{h}(E)$; dashed lines, $\bar{n}(E)$. (c,d) The time scales τ in the HH (c) and N62 (b) systems. Solid lines, $\tau_m(E)$; dash-dotted lines, $\tau_h(E)$; dashed lines, $\tau_n(E)$ in (c); and $0.01\tau_n(E)$ in (d).

In the original Hodgkin and Huxley paper [3], the transmembrane voltage V was measured with respect to the resting potential, and in the direction opposite to the one accepted later, so the variable V of Ref. [3] and the variable E in Eq. (1) are related by

$$E=-V$$

and the resting potential in the HH model corresponds to $E=0$ by definition; in fact, parameter E_l was not measured but chosen with a high precision to ensure that.

The N62 model was formulated in terms of true experimentally observed potentials. It was obtained by modifications of the HH system, taking into account the differences in the electrophysiology of the membrane of Purkinje cells in mammalian hearts from the membrane of the giant squid axon, known at that time. The most obvious change is a 100-fold increase in the value of $\tau_n(E)$, which corresponds to a much longer plateau of the action (pacemaker) potential duration in Purkinje cells compared to that in the nerve membrane. The differences between various voltage-dependent functions in these two models are illustrated in Fig. 1.

Figure 2 is the action and pacemaker potentials for the above system of equations (1). The HH action potential, i.e., the time course of the transmembrane voltage after a relatively small but overthreshold deviation from the stable resting state, has a triangular shape and relatively short duration. The N62 pacemaker potentials, i.e., the time course of the transmembrane potential during spontaneous oscillations, are much longer and have a more rectangular shape, with the characteristic ''overshot'' spikes labeled by *B*.

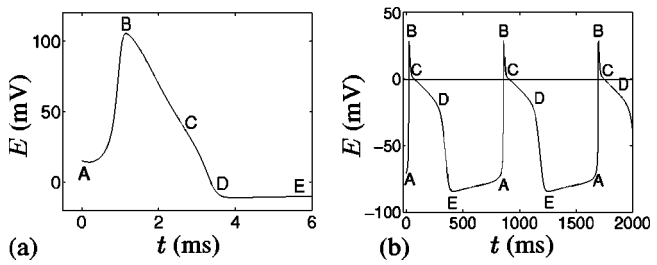

FIG. 2. (a) Action potential in the Hodgkin-Huxley system: solution for the initial point $(E,m,n,h)=(15,0.0530,0.5961,0.3177)$. (b) Pacemaker potential to Noble's system: solution for the initial point $(E,n,m,h)=(-70.6426,0.3276,0.0786,0.6025)$. The labels mark feature points of the graphs referred to in the asymptotic analysis to follow.

The difference in the morphology and in quantitative characteristics of the solutions of the two models is well understood physiologically. In this study, we aim to see what mathematical features of these systems provide for these differences, particularly the qualitative ones. Zeeman [1] suggested that this difference may be understood in terms of asymptotic properties of the underlying models considered as singularly perturbed ''fast-slow'' systems, and suggested two *a priori* model systems demonstrating the required features. In this study, we will use the same asymptotic approach as Zeeman did, but base the analysis on actual HH and N62 models. Although the asymptotic theory of fast-slow systems is well known (see, e.g., Ref. [13]), we give its brief overview in the following section, for reader's convenience and also to introduce the terms and notations we use later.

III. THE SINGULAR PERTURBATION THEORY OF THE FAST-SLOW SYSTEMS

We consider a system of k_1+k_2 first-order autonomous ordinary differential equations for k_1+k_2 dynamic variables, of which k_1 are ''slow'' and k_2 are ''fast.'' We denote the vector of slow variables $x_1\in\mathbb{R}^{k_1}$ and the vector of fast variables $x_2\in\mathbb{R}^{k_2}$. Then the system of equations is

$$\frac{dx_1}{dt}=f_1(x_1,x_2), \tag{2}$$

$$\epsilon\frac{dx_2}{dt}=f_2(x_1,x_2), \tag{3}$$

where $\epsilon>0$ is a small parameter. The transformation of time $t=\epsilon T$ brings this system to the form

$$\frac{dx_1}{dT}=\epsilon f_1(x_1,x_2), \tag{4}$$

$$\frac{dx_2}{dT}=f_2(x_1,x_2). \tag{5}$$

Systems (2), (3) (the slow-time system) and (4), (5) (the fast-time system) are equivalent to each other for every fixed $\epsilon>0$, but have different properties in the limit $\epsilon\to+0$.

The fast-time system at $\epsilon=0$ becomes

$$\frac{dx_1}{dT}=0, \tag{6}$$

$$\frac{dx_2}{dT}=f_2(x_1,x_2), \tag{7}$$

which means that the slow variables x_1 remain constant, and only the fast variables x_2 vary. A condition $x_1=x_1^0$ for a constant x_1^0 defines a k_2-dimensional manifold $\{(x_1^0,x_2)|x_2 \in \mathbb{R}^{k_2}\}$ in the phase space of the system $\{(x_1,x_2)\} = \mathbb{R}^{k_1+k_2}$. All such manifolds for all possible $x_1^0 \in \mathbb{R}^{k_1}$ fill the whole of the phase space $\mathbb{R}^{k_1+k_2}$. This k_1-parametric family of nonintersecting k_2-dimensional manifolds filling the whole (k_1+k_2)-dimensional space is called the *fast foliation* of that space, because it describes evolution of the system on the fast-time scale. Each of the manifolds $x_1=x_1^0$ makes a *leaf* of the fast foliation.

The slow-time system at $\epsilon=0$ becomes

$$\frac{dx_1}{dt}=f_1(x_1,x_2), \tag{8}$$

$$0=f_2(x_1,x_2), \tag{9}$$

i.e., a system of differential equations (8) with finite constraints Eq. (9). The finite constraints define a k_1-dimensional manifold in the (k_1+k_2)-dimensional phase space, which is called the *slow manifold*. This also defines the fast variables x_2 as implicit functions of the slow variables, $x_2=X(x_1)$, which reduces the original system of k_1+k_2 equations to the k_1 equations on the slow manifold, which can be written in the form

$$\frac{dx_1}{dt}=f_1(x_1,X(x_1)). \tag{10}$$

If the explicit solution of Eq. (9) in the form $x_2=X(x_1)$ is possible, i.e., if the slow variables x_1 can be chosen as coordinates on the slow manifold, the procedure is often called an *adiabatic elimination* of the fast variables x_2. Otherwise, the procedure still can be used, but another system of coordinates on the slow manifold is required.

The rigorous grounds for the asymptotic analysis of fast-slow systems have been laid down by classical theorems due to Tikhonov (1952) [14] and Pontryagin (1957) [15].

Tikhonov's theorem states conditions when a typical solution of the exact system starts with initial conditions at a point (x_1^0,x_2^0) demonstrating a "regular" behavior, which consists of two parts. The first part of a regular solution is a transient period lasting for the time interval $t\propto\epsilon$ or $T\propto 1$, close to the solution of Eq. (7) within the leaf $x_1=x_1^0$ starting from (x_1^0,x_2^0) and approaching the point $(x_1^0,X(x_1^0))$. The second part is slow motion along the slow manifold, it runs on the time scale $t\propto 1$ or $T\propto\epsilon^{-1}$ and the solution remains close to the solution of Eq. (10) with $x_2=X(x_1)$ with initial conditions $(x_1^0,X(x_1^0))$. Apart from the technical conditions, the essential assumptions for this regular behavior are that the slow part of the trajectory goes within an attracting region of the slow manifold, defined as set of equilibria of the fast subsystems Eq. (7) that are stable (attractive) in linear approximation, and that the initial point (x_1^0,x_2^0) is within the basin of attraction of the equilibrium $(x_1^0,X(x_1^0))$ in terms of the fast-time system (4), (5).

Pontryagin's theorem states conditions for the trajectories leaving off the slow manifold to start movement along the fast foliation. Typically, that happens when a trajectory moving along the slow manifold reaches the boundary of the attracting region of that manifold, provided that the slow trajectory is transversal to that boundary. If after taking off the slow manifold, the trajectory then happens to be in the basin of another stable part of the slow manifold, then, by Tikhonov's theorem, it will again have a quick transient along the fast foliation with subsequent slow motion along the slow manifold.

Thus, a trajectory with a regular behavior in a fast-slow system will consist of slow and fast pieces. Transition from fast to slow motion happens when a fast piece of trajectory reaches the slow manifold; and transition from slow to fast motion happens when a slow piece of trajectory reaches the boundary of the attracting region of the slow manifold. The slow pieces of trajectory are described by a system of k_1 differential equations, and the fast pieces are described by a system of k_2 differential equations. That means, both systems are simpler than the original system, thus may admit analytical solution, more exhaustive qualitative analysis, or at least be easier for numerical treatment, due to a smaller dimensionality and absence of the small parameter.

For the purposes of this paper, we will ignore some fine details that make life more complicated than the above idealized picture. E.g., the exact moment of the take-off at a small but fixed value of the small parameter depends on the initial conditions in a nontrivial way; namely, some very small fractions of trajectories continue to travel along the slow manifold well into the repelling region before taking off (so called "duck" solutions). A more detailed discussion of this and other related questions and a comprehensive bibliography can be found in Ref. [13].

Tikhonov [14] also presented a generalization of the reduction theorem, for hierarchical systems that depend on more than one small parameter, for instance,

$$\frac{dx_1}{dt}=f_1(x_1,x_2,x_3), \quad x_1 \in \mathbb{R}^{k_1},$$

$$\epsilon_1\frac{dx_2}{dt}=f_2(x_1,x_2,x_3), \quad x_2 \in \mathbb{R}^{k_2},$$

$$\epsilon_1\epsilon_2\frac{dx_3}{dt}=f_3(x_1,x_2,x_3), \quad x_3 \in \mathbb{R}^{k_3}, \tag{11}$$

where simultaneously $\epsilon_1\to+0$ and $\epsilon_2\to+0$. In this case, a typical trajectory would consist of (1) a superfast part when only x_3 change while x_1 and x_2 remain constant during time $t\propto\epsilon_1^{-1}\epsilon_2^{-1}$, followed by (2) a fast part when x_3 and x_2

change, so that $f_3(x_1,x_2,x_3)\approx 0$, while x_1 remain constant, lasting $t\propto \epsilon_1^{-1}$, followed by (3) slow motion when all three sets of variables change with $f_3(x_1,x_2,x_3)\approx 0$ and $f_2(x_1,x_2,x_3)\approx 0$, on the time scale $t\propto 1$.

We will say that system (2), (3) has *asymptotic structure* (k_1,k_2), and system (11) has asymptotic structure (k_1,k_2,k_3).

IV. THE TWO ZEEMAN'S MODELS

Zeeman [1] has considered two ''toy'' models, demonstrating two different types of asymptotic behavior of the shape of the action potential, which he believed resembled the shapes of the action potentials in nerve and in cardiac tissue. Thus, he called them the ''nerve'' model and the ''heart'' model. Without discussing how much these models actually relate to nerve or heart tissue, we briefly discuss them here, for the sake of introducing the key concepts and describing the method that we will subsequently apply to the HH and N62 systems.

Zeeman's heart model has asymptotic structure (1,1) and can be written in the form

$$\dot{b}=x-x_0,$$

$$\epsilon\dot{x}=-(x^3-x+b), \tag{12}$$

where b is the slow variable and x is the fast variable. This example is very similar to the famous system of equations due to FitzHugh [7]. The slow manifold of this system is a cubic parabola

$$f(x,b)=x^3-x+b=0.$$

The slow variable b cannot be chosen as a coordinate on this slow manifold, as this equation cannot be resolved with respect to the fast variable x. But it can be easily resolved with respect to b, and so x can be used as a coordinate.

The stable (attracting) regions on the slow manifold are defined by an additional condition that $\partial f/\partial x>0$ and the unstable (repelling) region corresponds to $\partial f/\partial x<0$. The boundary between these two regions satisfies the system of equations

$$f(x,b)=0,$$

$$\frac{\partial f}{\partial x}(x,b)=0,$$

which gives two solutions, $(x_1,b_1)=(1/\sqrt{3},2/3\sqrt{3})$ and $(x_2,b_2)=(-1/\sqrt{3},-2/3\sqrt{3})$. These are the *fold* points where the fast leaves are tangent to the slow manifold. At about these points, trajectories moving along the slow manifold would take off from it.

Since we have only one fast variable, the fast foliation is a family of lines $b=\text{const}$. In the leaves with $b\in(b_1,b_2)$ the fast subsystem has three equilibria, of which two are stable and separated by the unstable one.

The phase portrait of the system is shown in Fig. 3(a). The solid lines represent stable pieces of the slow manifold, defined by $x^3-x+b=0$ and $3x^2>1$, and the dashed line is the unstable piece, defined by $x^3-x+b=0$ and $3x^2<1$. They are separated by fold points shown by open circles. The fixed point (E) of the flow on the slow manifold is located on the attracting branch and therefore is stable.

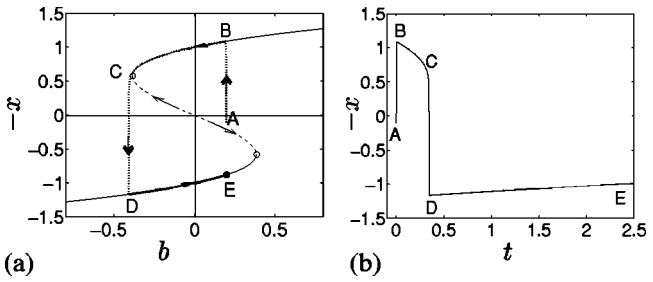

FIG. 3. (a) Phase portrait of Zeeman's heart model Eq. (12), $\epsilon=10^{-3}$. The double arrows represent the flow on the fast foliation and the single arrows represent the flow on the slow manifold. In this case, the slow manifold is the line $b=-x^3+x$. The dotted line represents the trajectory with the initial point $(b,x)=(0.2,0.1)$. (b) ''Action potential'' corresponding to the trajectory of panel (a) with the initial point $(b,x)=(0.2,0.1)$. Here the ''voltage'' is $-x$.

A selected trajectory is shown with dotted line and arrows. Starting from point A, it reaches the upper stable branch of the slow manifold (B), travels along it leftwards until reaching the left fold point (C) and cannot go any further as it has reached the repelling piece of the slow manifold. Therefore the trajectory has to make a jump from the fold point to the point D on the lower stable branch of the slow manifold, and then travel back along it to the stable equilibrium point E. Thus, trajectory $ABCDE$ represents a typical action potential. The AB part corresponds to the jump onset. The BC part represents the slow excitation part, the action potential plateau. The CD piece is the jump return, and DE is the smooth part of the return to the equilibrium. The corresponding action potential is shown in Fig. 3(b). It has a rather ''rectangular'' shape which was the reason Zeeman called it the heart model.

Zeeman's nerve model is a system with asymptotic structure (2,1):

$$\dot{a}=-2(a+x),$$

$$\dot{b}=-(a+1),$$

$$\epsilon\dot{x}=-(x^3+ax+b), \tag{13}$$

where a and b are the slow variables and x is the fast variable. The slow manifold is defined by the equation

$$f(x,a,b)=x^3+ax+b=0, \tag{14}$$

and the fast foliation is a two-parametric family of lines $a=\text{const}$, $b=\text{const}$. The *bistability* is observed for those a and b for which Eq. (14) has three real solutions for x; the set of such a and b is defined by condition $27b^2-4a^3>0$. On the contrary, if $27b^2-4a^3<0$, then Eq. (14) has one simple real solution for x, and we call this the *monostability* region on

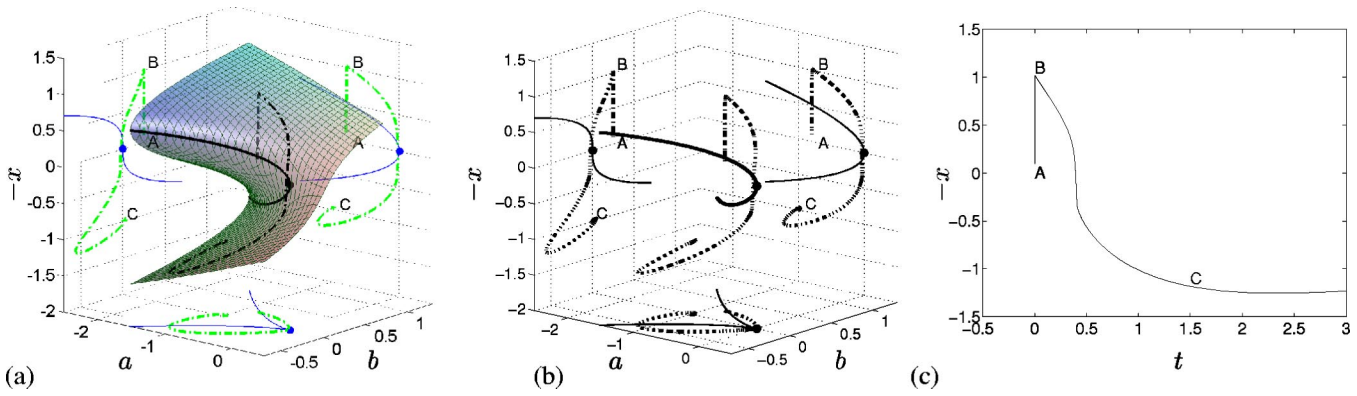

FIG. 4. (Color online) Phase portrait of Zeeman's "nerve" model Eq. (13), $\epsilon=10^{-3}$. The semitransparent surface is the slow manifold $x^3+ax+b=0$. The thick solid line is the fold line Eq. (17), the thin lines are its projections to the coordinate planes, the filled circles are the cusp point (0,0,0) and its projections. A selected trajectory, [initial conditions $(a,b,x)=(-0.8,0.25,-0.1)$] and its projections are shown by dash-dotted lines. (a) The slow manifold, trajectory and the fold curve, with their projections. (b) The trajectory and the fold curve with their projections, but without the slow manifold. (c) Action potential ("voltage" $-x$ vs time), corresponding to the trajectory of (a) and (b).

the (a,b) plane. The boundary between these regions in the (a,b) plane is the semicubic parabola

$$27b^2-4a^3=0, \tag{15}$$

which corresponds to one triple root [at point $(a,b)=(0,0)$] or one double and one simple roots (all other points) in Eq. (14).

Curve Eq. (15) is the projection onto the (a,b) plane of the *fold curve*, defined as the set of points where the slow manifold is tangent to the fast foliation, $(0,0,1)\cdot\nabla f(a,b,x)=\partial f/\partial x=0$. So the fold curves satisfy these two equations:

$$f(a,b,x)=0: \quad x^3+ax+b=0,$$

$$\frac{\partial f}{\partial x}(a,b,x)=0: \quad 3x^2+a=0,$$

and can be parametrized by x,

$$a=-3x^2, \tag{16}$$

$$b=2x^3. \tag{17}$$

This is a smooth curve in the (a,b,x) space. Its projection to (a,b) plane is also a smooth curve except where it is tangent to the direction of the projection, i.e., to the fast foliation. Such tangency is characterized by the third condition

$$\frac{\partial^2 f}{\partial x^2}(a,b,x)=0: \quad 6x=0.$$

Thus, the only point where this tangency happens in this model is the point (0,0,0) where Eq. (14) has a triple zero in x. This is the *cusp* (or *pleating*, by the terminology of Ref. [13]) point of the slow manifold.

The fold curve separates the stable (attracting) and unstable (repelling) regions of the slow manifold. Unlike the heart model, where the fold points have cut the slow manifold into three pieces, two stable and one unstable, here the fold curve only makes two pieces, one stable and one unstable. The unstable piece is projected onto the bistability region of the (a,b) plane, and corresponds to the middle root x of the corresponding functions $f(a,b,x)$. The stable piece includes the monostability region together with the upper and lower branches of the manifold over the bistability region.

The *resting state* in this model is $(a,b,x)=(-1,0,1)$ and it belongs to the upper ("recovery") branch of the stable part of the manifold over the stability region. Thus we have the excitable behavior: perturbations displacing the system from the resting state beyond the threshold, represented by the unstable branch of the slow manifold, fall down to the lower stable ("excitation") branch of the slow manifold, and return to the resting state from there. Unlike the heart model, now there are various opportunities. A trajectory can reach the fold line and make a jump return to the upper branch of the slow manifold moving towards the resting state, or it can reach that state moving entirely within the slow manifold, circumventing the cusp point, as now the upper and lower branches are connected to each other via the monostable region.

It is not possible to determine analytically, which of the two possibilities is realized for a given trajectory. The *phase portrait*, showing the slow manifold, the fold line, and a selected trajectory computed numerically, and a corresponding action potential are displayed in Fig. 4. This selected trajectory shows a marginal case: its return path goes very near to the cusp point. The corresponding action potential of this nerve model demonstrates a jump onset of excitation, but a moderately smooth return to equilibrium. This looks similar to the HH action potential, which was the reason Zeeman called this a nerve model. Note, however, that a small change in the initial conditions of the trajectory can result in a jump return, if the trajectory fails to go around the cusp.

V. PARAMETRIC EMBEDDING

We are going to apply the asymptotic procedure described above to the Hodgkin-Huxley and Noble (1962) systems of

equations defined by Eq. (1) and Table I. The immediate problem is that these systems do not depend on any parameters, but only contain constants, which have been measured experimentally and have certain values, even if not always known with a good precision.

Thus, to apply the singular perturbation technique, we need to introduce the small parameters artificially. This is, of course a standard practice in principle, often successfully used on intuitive basis. However, since this procedure is the key step in this study, we are going to formalize it, to avoid any ambiguity.

Definition 1. We will call a system

$$\dot{x} = F(x;\epsilon), \quad x \in \mathbb{R}^d,$$

depending on parameter ϵ, a *one-parametric embedding* of a system

$$\dot{x} = f(x), \quad x \in \mathbb{R}^d,$$

if $f(x) \equiv F(x,1)$ for all $x \in \mathbb{R}^d$. Similarly, we define an *n-parametric embedding*, with right-hand sides in the form $F(x,\epsilon_1,\ldots,\epsilon_n)$ and $F(x,1,\ldots,1) \equiv f(x)$. If an *n*-parametric embedding has a form of a Tikhonov's fast-slow system with asymptotic structure $(k_1,\ldots,k_n)$, we call it a *(Tikhonov)* $(k_1,\ldots,k_n)$*-asymptotic embedding.*

The typical use of this procedure has the form of a replacement of a small constant with a small parameter. If a system contains a dimensionless constant a which is ''much smaller than 1,'' then replacement of a with ϵa constitutes a one-parametric embedding; and then the limit $\epsilon \to 0$ can be considered. In practice, constant a would more often be replaced with parameter ϵ, but in the context of $\epsilon \to 0$ and $a = \text{const}$ this, of course, does not make any difference from ϵa.

There are infinitely many ways a given system can be parametrically embedded. In terms of asymptotics, which of the embeddings is ''better'' depends on the qualitative features of the original systems that need to be represented, or classes of solutions that need to be approximated. If a numerical simulation of the interesting properties can be done easily, then the practical recipe we use in this paper is to look at the solutions of the embedding at different, progressively decreasing values of the artificial small parameter ϵ, and see when the features of interest will start to converge. If the convergent behavior is satisfactorily similar to the original system with $\epsilon = 1$, the embedding is adequate for these features.

VI. ANALYSIS OF THE RELATIVE SPEED OF THE VARIABLES

To obtain the asymptotic embeddings of the two systems, we need to decide which variables shall be called slow and which shall be called fast. It is reasonable to decide that based on the characteristic times of those variables. The three gating variables have in their equations functions $\tau_{h,m,n}$ which have just that meaning. The equation for E does not have a function called τ_E, so we define the instant characteristic time of a variable j as the inverse of the corresponding diagonal element of the Jacobian of the right-hand sides,

$$\tau_j(E,h,m,n) = \left| \frac{\partial}{\partial j}\left(\frac{dj}{dt}\right) \right|^{-1}.$$

Obviously, for $j = h,m,n$ this gives the same functions τ_j as defined in Eq. (1), but also can be used for $j = E$. After that we decide that the variables with smaller τ will be called fast, and the variables with larger τ will be called slow.

These τ's are not constants, though, but functions, and these functions depend on different arguments, so they cannot be compared directly. To make them comparable, we consider typical solutions at selected initial conditions. This gives E, n, h, and m as functions of t, which, in turn, defines all the characteristic time scales of the variables, the τ's, as functions of t, via $\tau_j(t) = \tau_j(E(t),h(t),m(t),n(t))$, where $j = E$, h, n, or m.

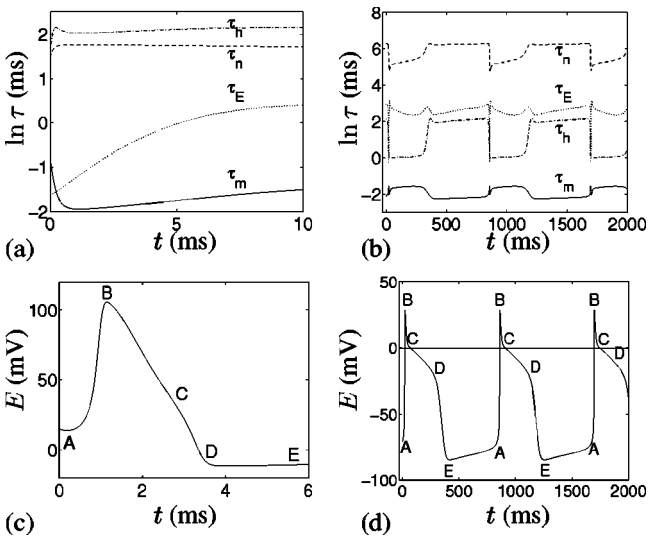

FIG. 5. (a,b) Graphs of $\tau_E(t)$ (dotted lines), $\tau_m(t)$ (solid lines), $\tau_n(t)$ (dashed lines), and $\tau_h(t)$ (dash-dotted lines), corresponding to the solutions $E(t)$ shown on (c,d) for (a,c) the HH and (b,d) N62 systems.

Figure 5(a) demonstrates that during the action potential in the HH model, variables E and m are always faster than variables h and n, and that, compared to each other, m is slower than E in the beginning of the action potential, but faster than E in the most part of the action potential. So we consider HH as a (2,2) system, with h and n as slow variables and E and m as fast variables.

Figure 5(b) shows that during the pacemaker potentials in the N62 model, m is always the fastest, that E and h interchange at around the overshot spikes, and that all three of these are always faster than n. So we consider N62 as a (1,2,1) system, where n is the slow variable, E and h are fast variables and m is the superfast variable.

VII. A (2,2)-ASYMPTOTIC EMBEDDING OF THE HODGKIN-HUXLEY SYSTEM

The above analysis suggests that the adequate asymptotic embedding of this system is $(2,2)$, with slow variables (h,n) and fast variables (E,m).

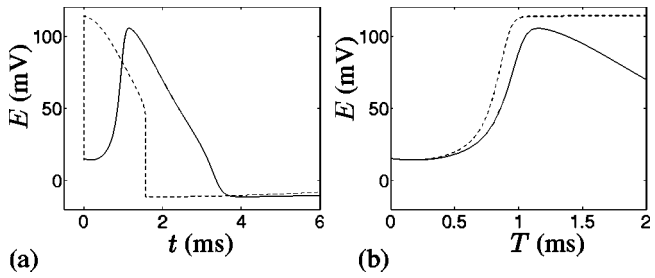

FIG. 6. The asymptotic embedding of the Hodgkin-Huxley system. (a) The action potentials in Eq. (18) with the initial condition $(E,m,h,n)=(15,0.0530,0.5961,0.3177)$, original system with $\epsilon=1$ (solid line), and with $\epsilon=10^{-3}$ (dashed line). (b) Same, in the fast time Eq. (19).

Thus, we consider the following one-parametric embedding of Eq. (1):

$$\frac{dn}{dt}=[\overline{n}(E)-n]/\tau_n(E),$$

$$\frac{dh}{dt}=[\overline{h}(E)-h]/\tau_h(E),$$

$$\epsilon\frac{dE}{dt}=C_M^{-1}f_E(E,h,m,n),$$

$$\epsilon\frac{dm}{dt}=[\overline{m}(E)-m]/\tau_m(E), \tag{18}$$

with one artificial small parameter ϵ. This embedding takes into account the real relationship between the characteristic time scales of dynamic variables during typical action potential solution. This system is singularly perturbed with respect to ϵ.

The corresponding system in the fast time $T=t/\epsilon$ is

$$\frac{dn}{dT}=\epsilon[\overline{n}(E)-n]/\tau_n(E),$$

$$\frac{dh}{dT}=\epsilon[\overline{h}(E)-h]/\tau_h(E),$$

$$\frac{dE}{dT}=C_M^{-1}f_E(E,h,m,n),$$

$$\frac{dm}{dT}=[\overline{m}(E)-m]/\tau_m(E), \tag{19}$$

which is regularly perturbed with respect to ϵ.

First we consider the limit $\epsilon\to+0$ numerically. The effect of this limit onto the shape of the action potential is shown in Fig. 6. We can see that the excitability of the model is preserved, and we observe the jump upstroke to the excited state, which becomes infinitely fast for infinitely small ϵ. However, the asymptotic embedding abolishes the smooth return to rest, as in the system with small ϵ, the return to rest includes a fast piece. This suggests that if this smooth return is essential, then the Tikhonov asymptotic embedding, contrary to Zeeman's expectation, is not sufficient, and one should consider some more adequate appearance of the small parameter(s) in the system. Note that this conclusion comes from the numeric experiment with the embedding, prior to, and thus independent of, any analytic work.

The slow manifold corresponding to embedding Eq. (18) is a two-dimensional manifold in the four-dimensional phase space $\mathbb{R}^4=\{(n,h,E,m)\}$. It is defined by equating the right-hand sides of the $\dot{m}$ and $\dot{E}$ equations to zero,

$$f_E(E,h,m,n)=0,$$

$$\overline{m}(E)-m=0.$$

This cannot be resolved explicitly with respect to the fast variables (E,m), but can be resolved with respect to (m,h), giving

$$m=\overline{m}(E),$$

$$h=h_{SM}(n,E)=-\frac{\overline{g}_{\mathrm{K}}(E_{\mathrm{K}}-E)n^4+\overline{g}_l(E_l-E)}{\overline{g}_{\mathrm{Na}}(E_{\mathrm{Na}}-E)\overline{m}^3(E)}. \tag{20}$$

This explicit representation of the slow manifold is convenient for visualization, and can be used to describe explicitly the slow motion in terms of (n,E) as coordinates on the slow manifold.

The fast foliation is a two-parameter set of planes $h=\mathrm{const}$ and $n=\mathrm{const}$ in $\mathbb{R}^4=\{(n,h,E,m)\}$. The flow within each of these planes is described by the system of two equations, which in the fast time $T=t/\epsilon$ state

$$\frac{dE}{dT}=C_M^{-1}f_E(E,h,m,n),$$

$$\frac{dm}{dT}=(\overline{m}-m)/\tau_m. \tag{21}$$

Some typical phase portraits of this system at selected values of parameters n and h are shown on Fig. 7. As anticipated from the formal speed analysis, which of the two variables is faster depends on their values, and the trajectories in the (m,E) phase plane can be almost vertical or almost horizontal in different parts of it. The system can have from one to three equilibria. The most typical picture observed during the selected action potential solution is the type shown in Fig. 7(b), with two stable equilibria and one unstable equilibrium. The trajectory starting from point labeled A represents the behavior similar to the onset of the action potential as shown in Figs. 2(a), 5(c), and 6, when the voltage experiences a period of stagnation or even a slight temporary decrease, before the m gates open up and allow the fast upstroke of the voltage.

The stable equilibria of all leaves constitute the attractive regions of the slow manifold. Let us describe the boundaries of these regions. We consider Eqs. (21) with n and h as constant parameters. The Jacobian of the right-hand sides of Eq. (21) at an equilibrium is

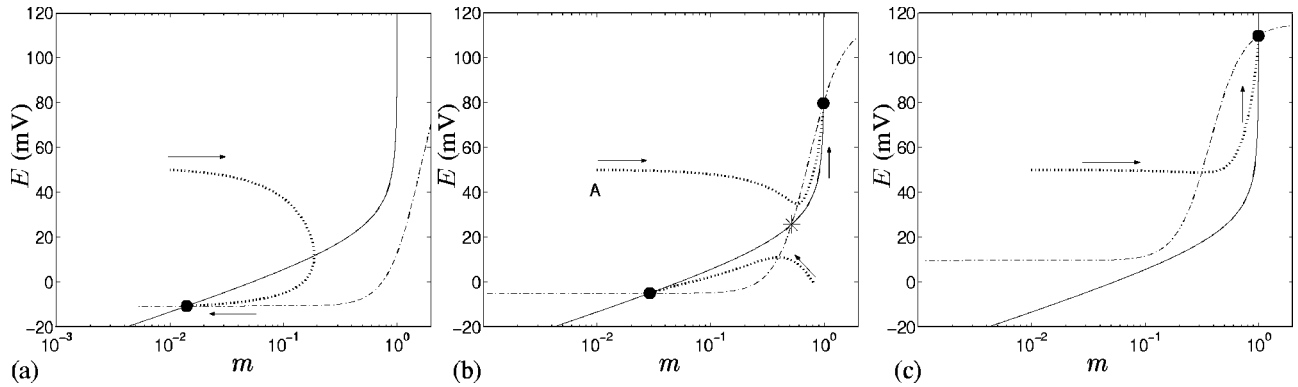

FIG. 7. Phase portraits of the fast subsystem equation (21) at selected values of parameters h and n: (a) $(n,h)=(0.61,0.01)$, (b) $(n,h)=(0.37,0.02)$, (c) $(n,h)=(0.14,0.05)$. Solid lines: the vertical null-clines $\dot{m}\propto\bar{m}(E)-m=0$. Dashed lines: the horizontal null-clines $\dot{E}\propto f(E,h,m,n)=0$. Filled circles: stable equilibria, asterisk: a saddle point. Dotted lines: selected trajectories.

$$J_{Em}=\frac{\partial(\dot{E},\dot{m})}{\partial(E,m)}=\begin{bmatrix} C_M^{-1}\partial f_E/\partial E & C_M^{-1}\partial f_E/\partial m \\ [\tau_m\bar{m}'-(\bar{m}-m)\tau_m']\tau_m^{-2} & -\tau_m^{-1}\end{bmatrix}.$$

However, since at an equilibrium $m=\bar{m}(E)$, this reduces to

$$J_{Em}=\begin{bmatrix} C_M^{-1}\partial f_E/\partial E & C_M^{-1}\partial f_E/\partial m \\ \bar{m}'\tau_m^{-1} & -\tau_m^{-1}\end{bmatrix}.$$

An equilibrium is stable in linear approximation if and only if $\mathrm{Tr}(J_{Em})<0$ and $\det(J_{Em})>0$. We have

$$\mathrm{Tr}(J_{Em})=C_M^{-1}\frac{\partial f_E}{\partial E}-\tau_m^{-1}$$
$$=-C_M^{-1}(\bar{g}_{\mathrm{K}}n^4+\bar{g}_{\mathrm{Na}}m^3h+\bar{g}_l)-\tau_m^{-1}<0, \quad (22)$$

for all physiologically sensible values of the variables, so the first stability condition is always satisfied. Further,

$$\det(J_{Em})=-C_M^{-1}\tau_m^{-1}\left(\frac{\partial f_E}{\partial E}+\frac{\partial f_E}{\partial m}\frac{d\bar{m}}{dE}\right), \quad (23)$$

and the zeros of this function determine the boundary of the attractive regions on the slow manifold. In terms of the structure of the phase portraits of the fast subsystems Eq. (21), condition $\det(J_{Em})=0$ can be viewed as $(\nabla\dot{E}\cdot\nabla\dot{m})=0$, i.e., tangency of the two null-clines at a double equilibrium. In terms of the geometry of the slow manifold, this condition means tangency of the fast flow to the slow manifold, i.e., defines the fold curves. In more detail, the fold curve satisfies the following three equations,

$$\dot{E}=0: \quad f_E(E,h,m,n)=0,$$

$$\dot{m}=0: \quad \bar{m}-m=0,$$

$$\det(J_{Em})=0: \quad F(E,m)\equiv\frac{\partial f_E}{\partial E}+\frac{\partial f_E}{\partial m}\frac{d\bar{m}}{dE}=0. \quad (24)$$

An explicit equation of the fold curve can be given if we choose E as a parameter. Then, resolving Eq. (23) with respect to h, m, and n, we get

$$h=\frac{\bar{g}_l}{\bar{g}_{\mathrm{Na}}}\frac{p(E)}{q_2(E)-\mu(E)},$$

$$m=\bar{m}(E),$$

$$n=\left(-\frac{\bar{g}_l}{\bar{g}_{\mathrm{K}}}\frac{q_1(E)-\mu(E)}{q_2(E)-\mu(E)}\right)^{1/4}, \quad (25)$$

where

$$\mu(E)=\bar{m}^3(E)/[\bar{m}^3(E)]',$$

$$p(E)=(E_l-E_k)(E_{\mathrm{Na}}-E_{\mathrm{K}})^{-1}/[\bar{m}^3(E)]',$$

$$q_1(E)=(E_{\mathrm{Na}}-E)(E-E_l)(E_{\mathrm{Na}}-E_l)^{-1},$$

$$q_2(E)=(E_{\mathrm{Na}}-E)(E-E_{\mathrm{K}})(E_{\mathrm{Na}}-E_K)^{-1}. \quad (26)$$

As n must be real, Eq. (25) only makes sense when $N(E)\equiv-[q_1(E)-\mu(E)]/[q_2(E)-\mu(E)]\geqslant 0$. The graph of functions $\mu(E)$ and $q_{1,2}(E)$ for the standard values of the parameters is shown in Fig. 8(a). There are two disjoint intervals,

$$E\in(-9.37\ldots,14.66\ldots)\cup(41.25\ldots,45.68\ldots),$$

in which $q_1(E)<\mu(E)<q_2(E)$ and thus $N(E)>0$. Thus, the fold curve consists of two disjoint branches.

The cusp point is defined by condition that system Eq. (21) has a triple equilibrium, or, equivalently, that the null-clines of that system have second-order tangency, or, equivalently, that the fold curve (24) is tangent to the fast leaves, i.e., planes $n=\mathrm{const}$, $h=\mathrm{const}$. This leads to the following condition, additional to the three equations Eq. (24):

$$\frac{\partial F}{\partial E}+\frac{\partial F}{\partial m}\frac{d\bar{m}}{dE}=0. \quad (27)$$

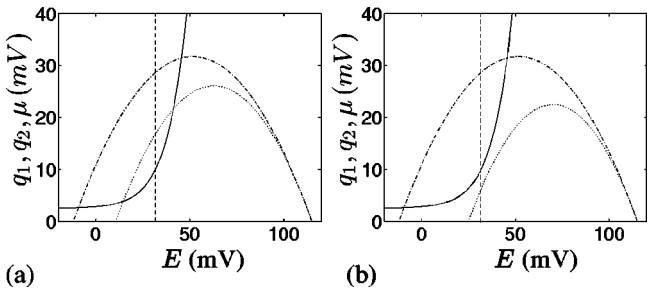

FIG. 8. Functions $q_1(E)$ (dots), $q_2(E)$ (dash dots), and $\mu(E)$ (solid) defined by Eq. (26) for (a) $E_l=10.613$ and (b) $E_l=25$. The fold line of the slow manifold corresponds to the values of E where $\mu(E)$ is between $q_1(E)$ and $q_2(E)$. Vertical dashed line is $E=E_*\approx 31.92$, corresponding to the cusp point.

Using the definition of $F(E)$, we find from here that the E coordinate of the cusp points, if any, is given by the inflexion points of the graph of the function $M(E)=(E-E_{\mathrm{Na}})\bar{m}^3(E)$. For the standard parameter values, there is only one such point, $E_*\approx 31.92$. The value of $N(E)$ at this point is negative, $N(E_*)\approx -0.021$. Therefore, the slow manifold at the standard parameter values does not have cusp points.

We now demonstrate that a variation of parameters in the HH system is possible that gives $N(E_*)>0$, so the slow manifold has a real cusp point. From Eq. (25) we can see that the sign of $N(E_*)$ depends on the relative location of the zeros of the functions $q_{1,2}(E)-\mu(E)$ to E_*. Note that the function $\mu(E)$ is determined by the properties of the activation gates of the Na channel, and variations of those are not physiologically feasible. On the contrary, the parameters E_{Na}, E_K, and E_l are determined by the ratios of the intracellular and extracellular concentrations of the corresponding ions, which can be changed during the experiments, and can vary physiologically depending on the ionic balance of the organism. From Fig. 8(b) one can see that the closest to the E_* root of $q_{1,2}(E)=\mu(E)$ is the left root of $q_1(E)$, obviously strongly correlated with the root of $q_1(E)=0$, i.e., $E=E_l$. Incidentally, as we noted above, E_l is the least reliable parameter of the model, as its value has not been measured, but chosen using indirect considerations. We have found that by changing E_l from its standard value of 10.613, we can shift the left zero of $q_1(E)-\mu(E)$ through $E_*=31.92$. Notably, this parameter variation does not involve function $M(E)$ whose inflexion point is E_*, so the value of E_* remains unchanged. Figure 8(b) shows what happens to q_1, q_2, and μ for $E_l=25$. We have $N(E)>0$ at the cusp point $E_*=31.92$. As a result, at $E_l=25$ and all other parameters at standard values, we have $N(E_*)\approx 0.0012>0$, and there is a cusp point, $(h,n,E,m)\approx(0.0013,0.1860,31.92,0.6711)$.

Note that the condition $N(E_*)>0$ is equivalent to the condition of having the single interval with $N(E)>0$, i.e., the slow manifold has a real cusp point if and only if the two fold lines join into a single fold line. This can be seen by considering the marginal case when the graphs of the functions $q_1(E)$ and $\mu(E)$ have a point of tangency; straightforward calculations show that this always happens at the point of the zero of the second derivative of $M(E)$, i.e., at E_*.

The phase portraits resulting from the above analysis for both values of E_l are shown in Fig. 9. As the phase space of the system is four dimensional, we depict only three-dimensional projections of the portraits. We use Eq. (20) to draw the slow manifolds, and Eq. (25) to draw the fold curves. Figure 9 also shows typical trajectories that go from a starting point (A) along the fast foliation until they reach the slow manifold (B), then along the slow manifold, until the fold curve (C), where we have a jump return down the fast foliation to the lower part of the slow manifold (D). Then the trajectories eventually move to the equilibrium point (E).

In the system with the modified value of E_l, there exists, theoretically, an alternative for the trajectories. Namely, with a different flow on the slow manifold, the trajectories could have returned to the equilibrium without a jump return, but only going along the slow manifold, around the cusp point, as they did in Zeeman's nerve model. However, as far as we could see, this possibility has not been realized in the HH model at any reasonable variations of parameters, and the action trajectories always have a jump return.

VIII. A (1,2,1)-ASYMPTOTIC EMBEDDING OF THE NOBLE (1962) SYSTEM

Our formal analysis of the relative speeds in the N62 model has shown that m is the fastest variable, E and h are of intermediate speeds comparable to each other, and n is the slowest variable. This understanding leads to the following (1,2,1)-asymptotic embedding:

$$\frac{dn}{dt}=[\bar{n}(E)-n]/\tau_n(E),$$

$$\epsilon_1\frac{dE}{dt}=C_M^{-1}f_E(E,h,m,n),$$

$$\epsilon_1\frac{dh}{dt}=[\bar{h}(E)-h]/\tau_h(E),$$

$$\epsilon_1\epsilon_2\frac{dm}{dt}=[\bar{m}(E)-m]/\tau_m(E). \tag{28}$$

First, we consider the limit $\epsilon_2\to 0$. The corresponding slow manifold is defined by equating the right-hand side of the $\dot{m}$ equation to zero, which gives m as a single-valued smooth function of E,

$$m=\bar{m}(E).$$

This makes m a uniquely and everywhere defined function of the slower variables, i.e., the slow manifold is uniquely and reversibly projected onto the (n,h,E) space. This slow manifold is always attractive. This allows adiabatic elimination of variable m from the system. Figure. 10 illustrates results of direct numerical simulations, illustrating the accuracy of this procedure. We see that the replacement of m with $\bar{m}(E)$ has virtually no effect on the shape of the action potential. In

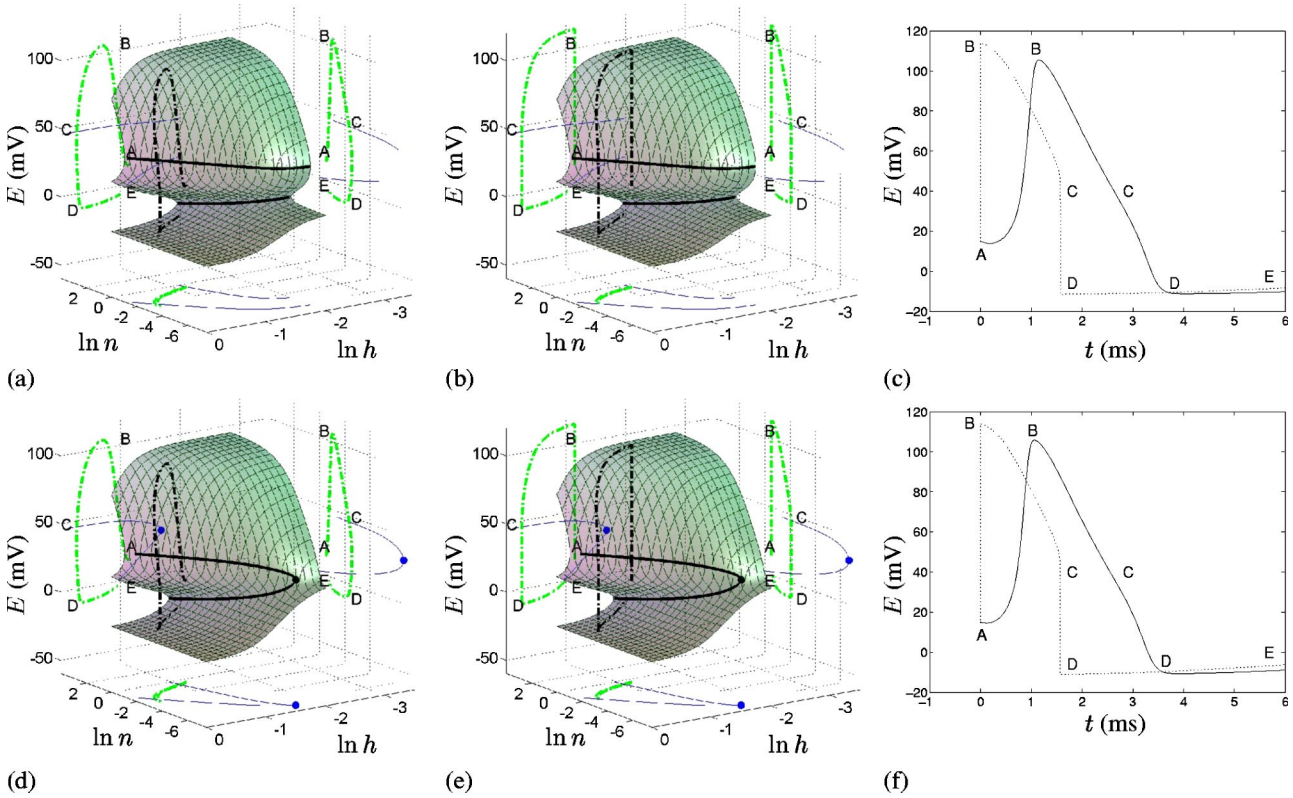

FIG. 9. (Color online) (a,d) The three-dimensional projections of the phase portraits of the Hodgkin-Huxley system and (b,e) its (2,2)-asymptotic embedding at $\epsilon=10^{-3}$, together with (c,f) corresponding action potentials, for (a,c) $E_l=10.613$ and (d,e) $E_l=25$. The semitransparent surface is the slow manifold Eq. (20). On (a,b,d,e), the thick solid lines are the fold curves and the thin solid lines are their projections on the coordinate planes $h=\text{const}$, $n=\text{const}$, and $E=\text{const}$. The trajectories and their projections are shown by dotted lines. The initial point of the trajectories is $(E,h,m,n)=(15,0.5961,0.0530,0.3177)$. The filled circle on (d,e) represents the cusp point $(E,h,m,n)=(31.92,0.0013,0.6711,0.1860)$. Labels $A-E$ mark the feature points of the solution on the coordinate planes $h=\text{const}$ and $n=\text{const}$ on (a,b,d,e) and are also marked on the graphs on (c,f).

other words, numerical experiment shows that variable m can be adiabatically eliminated from the system with good quantitative accuracy.

After this elimination, we have a (1,2) Tikhonov system,

$$\frac{dn}{dt}=[\bar{n}(E)-n]/\tau_n(E),$$

$$\epsilon_1\frac{dh}{dt}=[\bar{h}(E)-h]/\tau_h(E),$$

$$\epsilon_1\frac{dE}{dt}=C_M^{-1}\bar{f}_E(E,h,n), \tag{29}$$

where

$$\bar{f}_E(E,h,n)=f_E(E,h,\bar{m}(E),n).$$

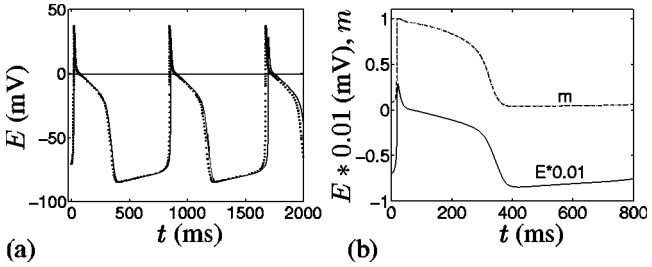

FIG. 10. The first asymptotic embedding in the Noble-1962 system Eq. (28) at $\epsilon_1=1$ and $\epsilon_2\to 0$, leading to adiabatic elimination of the gate m. (a) The pacemaker potentials in the original system, $\epsilon_2=1$ (solid line), and in the reduced system, $\epsilon_2=0$ (dotted line), for initial point $(n,E,h,m)=(0.3276,-70.6426,0.6025,0.0786)$. (b) The behavior of $m(t)$ (dashed line) and $\bar{m}(E(t))$ (dotted line) during one pacemaker potential [$E(t)\times 0.01$ shown by solid line for comparison]. The two curves $m(t)$ and $\bar{m}(E(t))$ are indistinguishable at this resolution.

This "reduced" system has two fast variables h and E and only one slow variable n. Therefore, the slow manifold is one dimensional, and the fast foliation is two dimensional. Thus, Zeeman's conjecture on the cusp singularity in the slow manifold is not applicable here even in theory, and we are bound to have a jump return.

This is confirmed by direct numerical simulations illustrated in Fig. 11(a). The pacemaker potentials in the system with small $\epsilon_1=0$ are somewhat shorter, mainly at the expense of the slow returns for $\epsilon_1=1$ becoming jump returns for $\epsilon_1\to 0$, and also by further quickening of the fast onsets.

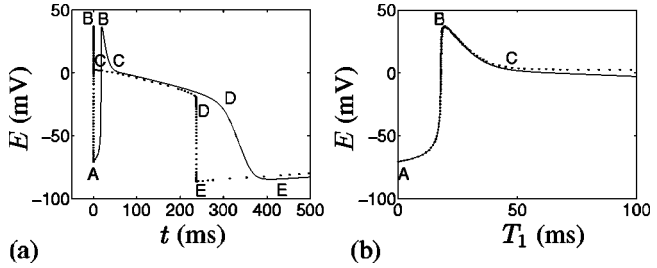

FIG. 11. The second asymptotic embedding in the Noble-1962 system Eq. (29) at $\epsilon_1 \to 0$. (a) Singular limit. Solid line: solution of the original system ($\epsilon_1 = 1$), dotted line, close to the reduced system ($\epsilon_1 = 10^{-3}$), for initial point $(n,E,h) = (0.3276, -70.6426, 0.6025)$. (b) The corresponding regular limit. Same initial conditions as in (a), in the fast time $T_1 = t/\epsilon_1$.

Correspondingly, the period of oscillations is shorter. Another observation can be made on the regular limit [Fig. 11(b)], i.e., the behavior of the system in the fast time: the overshot of the voltage at the onset of the pacemaker potential is due to the interaction of the two fast variables E and h, as it is preserved when the slow motion of n is frozen.

The one-dimensional slow manifold of Eq. (29) is defined by equations

$$h - \overline{h}(E) = 0,$$

$$\overline{f}_E(E,h,n) = 0.$$

This system of equations cannot be explicitly resolved with respect to (E,h), but is easily resolved with respect to (h,n), giving parametrization of the manifold by E,

$$h = \overline{h}(E),$$

$$\begin{aligned} n &= n_{SM}(E) \\ &= [\{(\overline{m^3 h g_{\mathrm{Na}}} + \overline{g}_{\mathrm{Na}_1})(E_{\mathrm{Na}} - E) + \overline{g}_{K_1}(E)(E_{\mathrm{K}} - E) \\ &\quad + \overline{g}_l(E_l - E)\}/\{\overline{g}_{\mathrm{K}}(E - E_{\mathrm{K}})\}]^{1/4}. \end{aligned}$$

The fast foliation consists of planes $n = \mathrm{const}$, with coordinates (h,E). The dynamics on the fast leaves in terms of the fast time T is described by the system

$$\frac{dE}{dT} = C_M^{-1} \overline{f}_E(E,h,n),$$

$$\frac{dh}{dT} = [\overline{h}(E) - h]/\tau_h(E), \tag{30}$$

where n is a constant parameter defining the leaf.

The stability of an equilibrium in the fast subsystem is determined by the Jacobian of the right-hand side of Eq. (30),

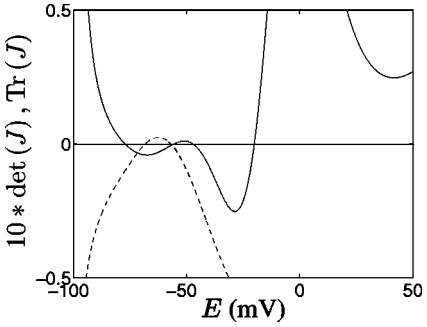

FIG. 12. Graphs of $10 \times \det J(E)$ (solid line, ms^{-2}) and $\mathrm{Tr}(J) \times (E)$ (dashed lines, ms^{-1}), where $J = J_{Eh}$ is defined by Eq. (31).

$$\begin{aligned} J_{Eh} &= \frac{\partial(\dot{E},\dot{h})}{\partial(E,h)} = \begin{bmatrix} C_M^{-1} \partial \overline{f}_E / \partial E & C_M^{-1} \partial \overline{f}_E / \partial h \\ [\tau_h \overline{h'} - (\overline{h} - h)\tau_h'] \tau_h^{-2} & -\tau_h^{-1} \end{bmatrix} \\ &= \begin{bmatrix} C_M^{-1} \partial \overline{f}_E / \partial E & C_M^{-1} \partial \overline{f}_E / \partial h \\ \tau_h^{-1} \overline{h'} & -\tau_h^{-1} \end{bmatrix} \end{aligned} \tag{31}$$

because $h = \overline{h}(E)$ at an equilibrium. The stability in linear approximation requires $\mathrm{Tr}(J_{Eh}) < 0$ and $\det(J_{Eh}) > 0$. We have

$$\mathrm{Tr}(J_{Eh}) = C_M^{-1} \frac{\partial \overline{f}_E}{\partial E} - \tau_h^{-1} = C_M^{-1} \left(\frac{\partial f_E}{\partial E} + \frac{\partial f_E}{\partial m} \frac{d\overline{m}}{dE} \right) - \tau_h^{-1}.$$

Unlike Eq. (22), we are not guaranteed that this function is negative in the physiological region, since $(\partial f_E/\partial m)(d\overline{m}/dE) > 0$. The graph of $\mathrm{Tr}(J_{Eh})(E)$ in the physiological range of E is shown in Fig. 12. It shows that stability condition $\mathrm{Tr}(J_{Eh})(E) < 0$ is violated in a range $E \in [E_{Tr}^1, E_{Tr}^2]$, where $E_{Tr}^1 \approx -68.25$, $E_{Tr}^2 \approx -57.01$.

Further,

$$\det(J_{Eh}) = -C_M^{-1} \tau_h^{-1} \left(\frac{\partial \overline{f}_E}{\partial E} + \frac{\partial \overline{f}_E}{\partial h} \frac{d\overline{h}}{dE} \right). \tag{32}$$

As can be seen from Fig. 12, condition $\det(J_{Eh}) < 0$ is satisfied in intervals $E \in (-\infty, E_{det}^1) \cup (E_{det}^2, E_{det}^3) \cup (E_{det}^4, +\infty)$, where $E_{det}^1 = -77.37$, $E_{det}^2 = -55.54$, $E_{det}^3 = -47.24$, $E_{det}^4 = -20.27$.

Thus, we see that the interval of instability due to the positive trace, (E_{Tr}^1, E_{Tr}^2), lies wholly inside the interval (E_{det}^1, E_{det}^2) where the equilibria are unstable due to negative determinant. Therefore, the stability of the equilibria of the fast subsystem, hence attractive and repelling pieces of the slow manifold, can be determined based on the sign of the determinant only, at least for the standard values of the parameters. And this criterion produces three disjoint attracting pieces of the slow manifold.

Incidentally, the sign of $\det(J_{Eh})$, and thus the stability of different parts of the slow manifold, can be deduced from the slope of its (n,E) projection. Indeed, this projection is defined by $n = n_{SM}(E)$, where

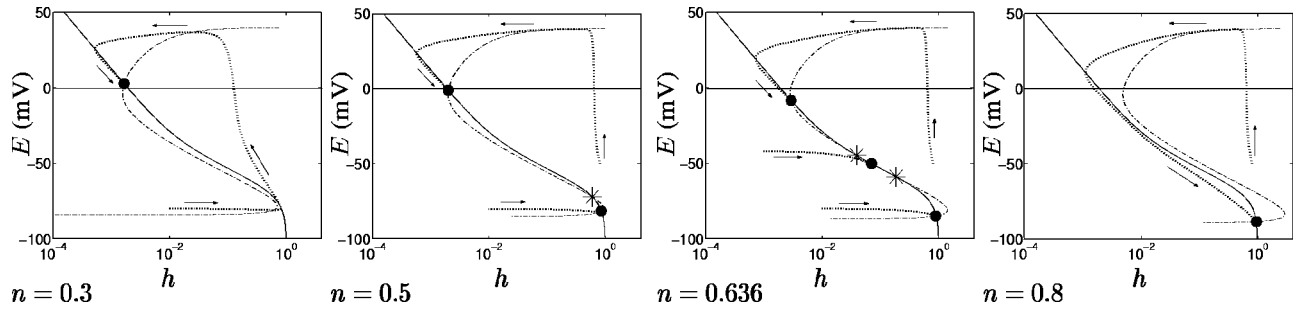

FIG. 13. Phase portraits of the fast leaves at the specified values of n. Dashed lines, the $\dot{E}=0$ isoclines; solid lines, $\dot{h}=0$ isoclines; dots, selected trajectories; filled points, stable equilibria; asterisks, saddle points.

$$\overline{f}_E(E,\overline{h}(E),n_{SM}(E))=0.$$

We differentiate $\overline{f}(E)$, and thus find the slope of the slow manifold projection as

$$\frac{dn_{SM}}{dE}=-\left(\frac{\partial\overline{f}_E(n)}{\partial n}\right)^{-1}\left(\frac{\partial\overline{f}_E}{\partial E}+\frac{\partial\overline{f}_E}{\partial h}\frac{d\overline{h}}{dE}\right).$$

Comparing this with Eq. (32) and noticing that

$$\frac{\partial\overline{f}_E(n)}{\partial n}=4\overline{g}_{\mathrm{K}}n^3(E_{\mathrm{K}}-E),$$

we see that $\det(J_{Eh})$ has the opposite sign to dn_{SM}/dE as long as $E>E_{\mathrm{K}}$, i.e., during any physiologically sensible action-pacemaker potential.

Thus, the stable points of the slow manifold are those where the slope of the projection of the slow manifold to the (E,n) plane, see Figs. 14(a,b), is negative.

Figure 13 shows the different types of phase portraits of the fast subsystem, taken at selected values of n. These portraits illustrate the null-clines, equilibria, and selected trajectories. In Fig. 14, one can see also the projection of the slow manifold and the selected trajectory to the (n,E) plane, for the original system, $\epsilon_1=1$ [panel (a)] and for the reduced system $\epsilon_1\to+0$, represented by $\epsilon_1=10^{-3}$ [panel (b)].

The selected trajectory, representing the pacemaker potential, has slow motion pieces along the upper (CD) and lower (EA) branches of the slow manifold. Between these slow motions, there are fast transitions from the lower branch to the upper branch (ABC), which is the jump onset with an overshot of the pacemaker potential, and from the upper branch to the lower branch (DE), which is the jump return. These fast transitions occur near the fold points on the slow manifold. The labels A–E correspond to the feature points of the pacemaker potentials shown in Fig. 2. This fast-slow behavior is exaggerated on panel (b) where the fast pieces of trajectory are visually vertical.

The pacemaker potential trajectory does not ever come close to the intermediate stable branch of the slow manifold. As can be seen from Fig. 13(c), the angle between the null-clines at the middle stable equilibria of the fast subsystem is very small and the stability of these equilibria must be very weak. Indeed, the numerical experiment shows that at $\epsilon_1=1$, there are no trajectories that would stay along the middle branch of the slow manifold for any considerable time.

Note that there is no stable equilibrium in the model at the standard parameter values, and so the selected trajectory represents auto-oscillations. With this fact in mind, the overall behavior is comparable to that of Zeeman's heart model in an appropriate parameter region that gives limit cycle behavior. The only essential difference in the morphology of the pace-

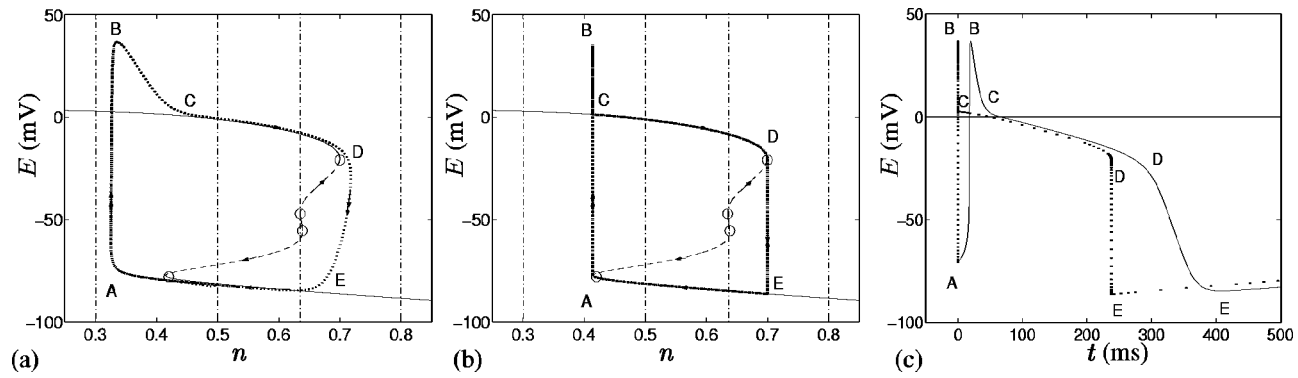

FIG. 14. (a) The projection of the phase portrait of the N62 system onto the (n,E) plane. Solid and dashed lines: the slow manifold. Dotted line: a selected ''pacemaker potential'' trajectory. Vertical dot-dashed lines: positions of the selected fast leaves shown in Fig. 13 (b) Same as (a), with the trajectory of the embedded system at $\epsilon_1=10^{-3}$. (c) The pacemaker potentials of the original (solid line) and embedded (dotted line) systems. Letters *A, B, C, D, E* mark feature points of the pacemaker potential trajectory.

maker potential is the nonmonotonic onset, represented by the *ABC* piece of the trajectory, including the overshot. This nonmonotonicity is a consequence of the behavior of trajectories in the corresponding two-dimensional fast subsystem, as illustrated by the portrait on the fast leaf $n=0.3$, Fig. 13(a). This is essentially different from what is possible in one-dimensional fast subsystems, where the transition is always monotonic.

IX. DISCUSSION

We have analyzed the asymptotic behavior of two classical models of biological excitable systems, the Hodgkin-Huxley (HH) model of a nerve axon and Noble-1962 (N62) model of a heart muscle fibre. Although the latter was only a modification of the former, we have found that their asymptotic properties differ substantially. The least surprising difference is the longer duration of the pacemaker potentials in the N62 model than the action potentials in the HH model, as it is a direct consequence of the speed of the slow potassium current decreased by the two orders of magnitude in N62 compared to HH. However, the differences do not stop there.

First of all, the asymptotic structure of the two models is different: whereas the HH model is a (2,2) model, i.e., has two slow and two fast variables, the N62 model is a (1,2,1) model, i.e., has 1 slow, 2 fast, and 1 superfast variable. By virtue of the simple structure of the superfast system, which always has a unique and stable equilibrium, the N62 model is readily reduced to a (1,2) system, with one slow variable and two fast variables. After that, the HH and N62 models have a common feature, which makes them different from the two Zeeman's models: two fast variables in both HH and reduced N62, as opposed to one fast variable in both Zeeman's heart and nerve models. This feature appears to be not just a technical difference, but brings about new phenomena that are not possible in systems with one fast variable. In the HH model, the feature we found is less prominent: it is a slight delay of the fast onset of the action potential, even with its slight decrease in the beginning. In the N62 model, this is much more prominent: it is the overshot in the beginning of a pacemaker potential. This last feature is quite typical of many cardiac excitability models and of real cardiac cell's behavior; thus, we believe that the mechanism of the overshot in the N62 model may be prototypical for more detailed and up-to-date models. An important lesson here is that if any asymptotic embeddings in such models are to retain this property, they *must* have at least a two-dimensional fast foliation.

Another characteristic feature of the solution is the ''return,'' i.e., the repolarization to the resting potential in the excitable HH system and to the lower phase of oscillations in the oscillatory N62 model. The two Zeeman's models differ in that the nerve model, at appropriate initial conditions, has a smooth return, while the heart model always has a jump return. In our analysis, both the HH nerve and N62 heart models have proved to demonstrate jump returns. However, the reasons for that are different in the two models. In the N62 model, there is only one slow variable, thus the slow manifold is only one dimensional, and therefore, in accordance with Zeeman's reasoning, the slow return is impossible. Indeed, the action and resting branches of the slow manifold have been found to be separated in the phase space. In contrast, the HH model has two slow variables, and a two-dimensional slow manifold. Therefore, there exists a theoretical possibility of this manifold to have a cusp catastrophe in its mapping to the space of slow variables, and a possibility for trajectories to return from the upper to the lower branch of the slow manifold by going along that manifold around the cusp point. Indeed, we have found that, although such a catastrophe is not observed in the model at the standard values of the parameters, it may appear at appropriate, physiologically feasible variations of the parameters. However, the existence of this catastrophe does not automatically imply that trajectories will necessary go around the cusp point, and as the numerical calculations show, in fact they do not, at least at the parameter values studied.

Notice that the very fact of the jump return does not depend on details of the analytic work, but is a direct result of the chosen parametric embedding, i.e., the way the artificial small parameter is introduced in the model to make asymptotic analysis possible. Indeed, this property can be established by direct numerical calculations of trajectories in systems with progressively decreasing values of the artificial parameter. This is a convenient way to establish properties of an asymptotic embedding, *prior to* the asymptotic analysis of that embedding.

Applied to the character of the return in the HH and N62 models, the present results are less than entirely agreeing with intuitive impressions that one might have observing the solutions of the original models. Indeed, the action potential in the HH model definitely looks more triangular than rectangular, which was the original impulse for Zeeman's conjecture on the role of the cusp catastrophe. And yet, this property is not conserved in the asymptotic embedding. The pacemaker potentials in the N62 model are less triangular, and the question of whether the return to the lower potential should be considered fast or slow may be a subjective matter. It is, however, certain that the slope of the return is much smaller than the slope of the onset. In the asymptotic embedding considered, more specifically, in the limit $\epsilon_1 \to +0$, this difference is not reflected at all, and both slopes become vertical.

Thus, we conclude that if the slow character of the return is of importance, then the asymptotic embedding we used here should be considered unsatisfactory. At this point, we should recall that there are infinitely many asymptotic embeddings, i.e., infinitely many ways artificial small parameter(s) can be introduced to a given system of equations. The asymptotic embeddings we used here were both of the Tikhonov fast-slow-type, where small parameters appear as factors at some of the time derivatives, or as factors at some of the right-hand sides, depending on the choice of the time scale. The number of ways such embeddings can be done for a system of only a few equations is limited, and considering the formal speed analysis that we performed in Sec. VI, there are practically no alternatives [19]. This class of perturbed systems is the best studied, and a huge amount of literature

dedicated to singular perturbations and fast-slow systems is practically restricted to this class: e.g., it is *the only* class considered in a very comprehensive review [13]. Thus, the formal analysis of asymptotic properties of realistic excitable systems ought to have started with this embedding. However, we now see that analysis restricted to this class may not be sufficient, and other types of embedding should be considered. And this may involve interesting mathematical questions, as the mathematical theory of non-Tikhonov fast-slow systems is very little developed yet.

There are two more points to notice in the analysis of the N62 model, the possibility of fast oscillatory instability and middle stable branch of the slow manifold. Oscillatory instability is impossible in systems with one fast variable, but is theoretically possible in systems with two fast variables, and would be characterized by change of sign of the trace of the Jacobian at the equilibrium at a positive determinant of the Jacobian, i.e., a Hopf bifurcation. This possibility is not realised in the N62 model, as the change of sign of the trace happens at negative determinant; however, the fact that such a change happens is suggestive of the fact that this kind of instability may take place in this system at different parameter values, or in other models of similar nature. This would correspond to bursts of high frequency oscillations on the wake of the action-pacemaker potential; indeed, such bursts are observed in some models [16]. The middle stable branch in N62 model was completely unexpected. If it was more pronounced, it could correspond, e.g., to other ''minor'' action potentials with smaller amplitude and much shorter duration than the normal potentials. This possibility is not realized in the N62 system at normal parameter values, and so could be considered as an artifact of the parametric embedding. But again, the fact that such a feature takes place albeit formally, suggests that in some similar systems it may appear indeed. We are not aware of any theoretical or reliable experimental description that could be associated with such minor potentials; however, there are certain experimental facts which do not yet have firm theoretical explanations, and for which such minor potential explanation may look plausible [17].

ACKNOWLEDGMENTS

V.N.B. is grateful to D. Barkley and I.V. Biktasheva for encouraging discussions. This work was supported in part by EPSRC.

[1] E.C. Zeeman, *Differential Equations for the Heartbeat and Nerve Impulse* (Mathematics Institute, University Of Warwick, Coventry, 1972).
[2] E. C. Zeeman, *Catastrophe Theory. Selected Papers 1972–1977* (Addison-Wesley, Reading, MA, 1977).
[3] A.L. Hodgkin and A.F. Huxley, J. Physiol. (London) **117**, 500 (1952).
[4] D. Noble, J. Physiol. (London) **160**, 317 (1962).
[5] E. Marder and A.A. Prinz, BioEssays **24**, 1145 (2002).
[6] D. Noble, BioEssays **24**, 1155 (2002).
[7] R. FitzHugh, Biophys. J. **1**, 445 (1961).
[8] V.I. Krinsky and Y.M. Kokoz, Biofizika **18**, 506 (1973).
[9] R.R. Aliev and A.V. Panfilov, Chaos, Solitons Fractals **7**, 293 (1996).
[10] F. Fenton and A. Karma, Chaos **8**, 20 (1998).
[11] G. Duckett and D. Barkley, Phys. Rev. Lett. **85**, 884 (2000).
[12] O. Bernus, R. Wilders, C.W. Zemlin, H. Verschelde, and A.V. Panfilov, Am. J. Physiol. **282**, H2296 (2002).
[13] V.I. Arnol'd, V.S. Afrajmovich, Y.S. Il'yashenko, and L.P. Shil'nikov, in *Dynamical Systems V*, edited by V.I. Arnol'd (Springer-Verlag, Berlin, 1994), Chap. 4.
[14] A.N. Tikhonov, Mat. Sb. **31**, 575 (1952).
[15] L.S. Pontryagin, Izv. Ross. Akad. Nauk, Ser. Math. **21**, 107 (1957).
[16] G.S. Cymbalyuk, Q. Gaudry, M.A. Masino, and R.L. Calabrese, J. Neurosci. **22**, 10 580 (2002).
[17] R.R. Aliev, F. Baudenbacher, P. Baudenbacher, and J.P. Wikswo (unpublished).
[18] R. Suckley and V. N. Biktashev, Int. J. Bifurcation Chaos Appl. Sci. Eng. (to be published).
[19] Note, however, our previous analysis of a (2,1,1) Tikhonov embedding of the HH system [18], which delivered results very similar to the results presented here. Our attempts to do other types of Tikhonov embeddings to these two systems were less encouraging, as the most important properties, such as the excitability, were not preserved.